Influence of light pattern thickness on moving behaviors of dielectric microparticles manipulated by optoelectronic tweezers

Shuailong Zhang,[1,1,2,3,4*] Mohamed Elsayed,[3,4] Yujie Chen,[5] Yanfeng Zhang,[5] Steven L. Neale,[6] and Aaron R. Wheeler[3,3,4*]

1. *School of Mechatronical Engineering, Beijing Institute of Technology, Beijing, 100081, China*
2. *Beijing Advanced Innovation Center for Intelligent Robots and Systems, Beijing Institute of Technology, Beijing, 100081, China*
3. *Department of Chemistry, University of Toronto, Toronto, Ontario, M5S 3H6, Canada*
4. *Institute of Biomedical Engineering, University of Toronto, Toronto, Ontario, M5S 3G9, Canada*
5. *Donnelly Centre for Cellular and Biomolecular Research, University of Toronto, 160 College Street, Toronto, ON M5S 3E1, Canada.*
6. *State Key Laboratory of Optoelectronic Materials and Technologies, School of Electronics and Information Technology, Sun Yat-sen University, Guangzhou, 510275, China*
7. *James Watt School of Engineering, University of Glasgow, Glasgow, G12 8QQ, United Kingdom*

Author email addresses:

Shuailong Zhang: shuailong.zhang@bit.edu.cn ;

Mohamed Elsayed: mohammed.elsayed@mail.utoronto.ca;

Yujie Chen: chenyj69@mail.sysu.edu.cn;

Yanfeng Zhang: zhangyf33@mail.sysu.edu.cn;

Steven L. Neale: Steven.Neale@gla.ac.uk;

Aaron R. Wheeler: aaron.wheeler@utoronto.ca;

Contact details for the corresponding authors:

Shuailong Zhang

Email: shuailong.zhang@bit.edu.cn; Tel: 010-689865711

Address: School of Mechatronical Engineering, Beijing Institute of Technology, 5 Zhongguancun St, Haidian District, Beijing, 100081, China.

Aaron R. Wheeler

Email: aaron.wheeler@utoronto.ca; Tel: 1-416-946-3866; Fax: 416-946-3865

Address: 80 St. George Street, Department of Chemistry, University of Toronto, Toronto, ON, Canada M5S 3H6.

Abstract

Optoelectronic tweezers (OET) is a useful optical micromanipulation technology that has been demonstrated for many useful applications. In this work, we studied the use of light patterns with different shapes and thickness to manipulate dielectric microparticles with OET. It was demonstrate that the maximum velocities of the microparticles increase to a peak and then gradually decrease as the light

pattern's thickness increases. Numerical simulations were run to clarify the underlying physical mechanisms and it was demonstrated that the observed phenomenon is due to co-influence of horizontal and vertical DEP forces related to light pattern's thickness. Further experiments were run on light patterns with different shapes and objects with different sizes and structures. The experimental results indicate that the physical mechanism elucidated in this research is a universal one that applies for different light pattern shapes and different objects, which is useful for enabling users to optimize OET settings for various micromanipulation applications in future.

Key words: Optoelectronic tweezers, optical micromanipulation, dielectrophoresis, microparticle, micromotor

Optoelectronic tweezers (OET) is an optical micromanipulation technology that relies on optically-induced-dielectrophoresis (ODEP) force for the control and actuation of micro-/nano-scale objects.[1-5] Based on light patterned electric fields, OET is capable of exerting pico-to-nano Newton manipulation forces,[6,7] and is well suited for parallel and independent control of multiple objects.[1,3,8,9] Because of these outstanding micromanipulation capabilities, OET has been widely used to manipulate and assemble bio-analytes and molecules,[10-12] cells of different species,[13-20] nano-/micro- particles,[8,21-25] electronic/photonic components,[26-32] and microrobots,[9] thus offering a useful scientific tool to investigate microscopic world for physical, chemical and biological studies. More recently, OET technology has been successfully commercialized and used in the biopharmaceutical industry for antibody discovery and cell therapy development,[33] demonstrating the prospect of this technology in both research and industrial settings.

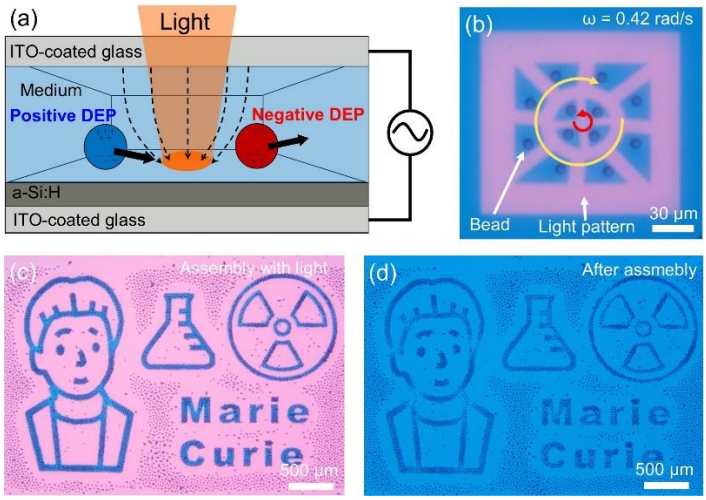

Figure 1. (a) Schematic of an OET device, in which microparticles are manipulated via positive or negative DEP forces. (b) A video frame showing the use of dynamic light pattern to move/rotate multiple 10 μm polystyrene microbeads at an angular velocity of 0.42 rad/s. Red and yellow arrows represent the counter-clockwise and clockwise rotational directions of the microbeads in the central and surrounding regions, respectively. See Supplementary Video 1 (clip 1) for more details. (c) Microscope image

showing the illumination of the microbead suspension with a light pattern depicting a stylized caricature of Marie Curie with symbols of Erlenmeyer flask and radiation. (d) Microscope image of the OET-assembled micropattern. See Supplementary Video 1 (clip 2) for more details.

In an OET system, light pattern is a key factor that influences the moving behaviors of the controlled micro-objects. Previous studies have shown that both the wavelength and optical intensity of light pattern can influence the performance of OET for particle manipulation.[34,35] However, for a standard OET system with given light sources, there is little room to adjust the properties of light sources to optimize the performance of OET. Since OET is based on ODEP forces, the distribution of light patterned electric field has a big influence on the moving behaviors of micro-objects. Therefore, in this work, we studied the influence of different-shaped light patterns and their thickness on the moving behaviors of microparticles and clarified the underlying physical mechanisms for the observed phenomenon. This is important for enabling users to optimize OET settings for efficient manipulation of micro-objects. Simulations in COMSOL Multiphysics (COMSOL Inc., USA) were carried out to clarify the experimental results and provide insights to the physical mechanisms. It was demonstrated that thicker light patterns can induce stronger electric field gradient in the horizontal plane, exerting stronger horizontal DEP forces and thus a higher moving velocity for the microparticles. However, light patterns beyond certain thickness can increase the DEP force in the vertical plane, making the microparticles escape from the OET trap at a lower moving velocity. Therefore, two physical mechanisms should be considered when choosing the rightful parameters for light patterns to achieve best OET performance for micromanipulation.

Shown in Figure 1(a) is a schematic of an OET device, compromising two plates. The top plate is an indium tin oxide (ITO)-coated glass slide; the bottom plate is also an ITO-coated glass slide, but deposited with an additional photoconductive layer of hydrogenated-amorphous-silicon (a-Si:H). The two plates were mounted together via a 150-μm-thick spacer to form a microchamber, in which the micromanipulation was performed. When a bias voltage is applied between the two plates and a light pattern is projected on the a-Si:H layer, a non-uniform electric field is generated in the liquid microchamber, which interacts with the micro-objects and produces DEP forces. If the micro-object is more polarizable than the surrounding medium [i.e. the real part of the Clausius-Mossotti (CM) factor is above 0], it will be attracted to the illuminated region due to positive DEP force; if the micro-object is less polarizable than the surrounding medium (i.e. the real part of the CM factor is below 0), it will be repelled from the illuminated region due to negative DEP force.[36] In this work, 10 μm spherical polystyrene microbeads (Polysciences Inc., USA) were used, which were suspended in deionized water containing “Tween 20” (0.05% v/v) and pipetted into the microchamber of the OET device. The OET device was driven by an AC potential (10 Vpp 20 kHz square wave). On applying the AC voltage, the polystyrene beads were repelled by the illuminated region due to negative DEP force, allowing the use of hollow light patterns consisting of illuminated and dark regions to move and rotate the beads, as shown in Figure 1(b) and Supplementary Video 1 (clip 1). Besides, when a static light pattern is projected

[Figure 1 (c)], the microbeads were repelled from the illuminated region and accumulated at the dark region, forming desired micropattern [Figure 1(d)] featuring the used light pattern. More details can be found in Supplementary Video 1 (clip 2). These results demonstrate the versatility of the OET technology for microparticle manipulation based on different light patterns, and also highlights the importance to investigate the influence of different light pattern parameters on electric field distribution and related microparticle's moving behaviors in an OET system.

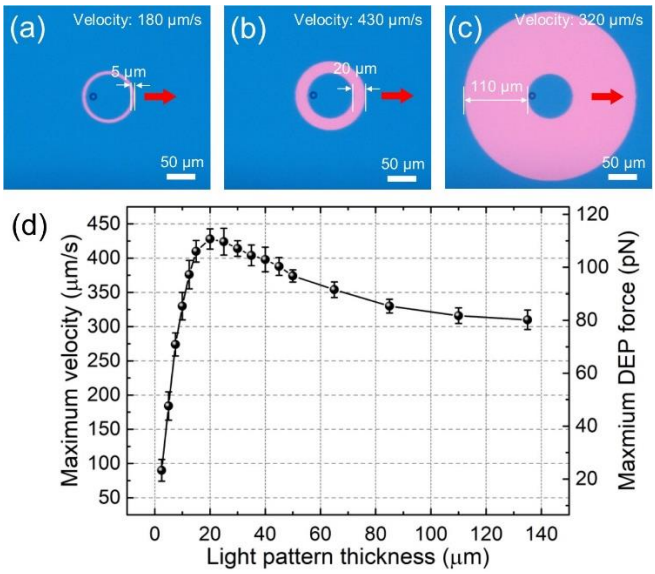

Figure 2. (a)-(c) Microscope images of a 10 μm polystyrene microbead trapped by "doughnut"-shaped light patterns with the same inner diameter but different ring thickness (i.e. 5 μm, 20 μm and 110 μm), and moving at 180 μm/s, 430 μm/s and 320 μm/s, respectively. See Supplementary Video 2 for more details. Red arrow represents the moving direction. (d) Maximum velocity and maximum DEP force versus light pattern's ring thickness. Error bars represent standard deviation for five replicates.

To investigate the influence of light pattern on microparticle's moving behavior, a single 10-μm-diameter bead was trapped by "doughnut"-shaped light patterns with fixed inner diameter at 80 μm but different ring thickness, as shown in Figure 2(a)-(c) and Supplementary Video 2 (worth noting that "doughnut"-shape is the most widely used light pattern shape for OET manipulation). In this case, the light pattern was kept stationary while the motorized stage was programmed to move linearly, and the maximum moving velocity of the bead was measured by gradually increasing the speed of the motorized stage until the bead fell out of the trap. Using this method, the maximum moving velocities of the bead manipulated by light patterns with different ring thickness were measured. As shown in Figure 2(d), the maximum moving velocity of the bead increases rapidly to a peak and then slightly decreases as the ring thickness increases from 2.5 μm to 135 μm. According to Stoke's law, the DEP actuation force exerted on the bead is equal to the viscous drag force,[7,17,24,37] i.e:

$$F_{DEP} = F_{drag} = 6\pi\eta r v \qquad (1.)$$

where η is the viscosity of the liquid, r is the radius of the bead and v is velocity of the bead. Since gravity forced the bead to sit in proximity to the a-Si:H surface, Faxen's correction needs to be applied

to adjust the calculation of the viscous drag force and the DEP force.[6,17,37] Therefore, the maximum DEP force exerted on a single bead can be calculated for the "doughnut"-shaped light pattern with different ring thickness, as shown in Figure 2(d). These experimental results demonstrate the influence of light pattern thickness on the moving behaviors of microparticles under OET manipulation.

To clarify the physical mechanism for the observed experimental results, simulations were carried out in COMSOL Multiphysics based on a 2D simulation model. The model length (X axis) and height (Y axis) were set to 500 μm and 150 μm, respectively. The OET trap created by the "doughnut"-shaped light pattern is located at the bottom of the model, with its inner diameter set to 80 μm and thickness set to different values used in the experiment (using the parameter sweep function). Other simulation parameters (voltage, frequency, medium conductivity, etc.) were set according to the actual experimental parameters. To simulate the electric potential distribution, an AC/DC module of COMSOL Multiphysics was applied and specific boundary conditions were implemented for the simulation model. In this work, electric insulation was set for the sides of the model and the top side of the model was set as ground (0 V), while the bottom side of the model was given an electric potential of 10 V. Different parts in the simulation model were defined as sub-domains and the interfaces between different sub-domains were set to continuity boundary condition. Then, the electric potential and electric field was computed by solving the continuity equations:

$$\nabla \cdot J = Q_{j,v} \tag{2.}$$

$$J = \sigma E + j\omega D + J_e \tag{3.}$$

$$E = -\nabla V \tag{4.}$$

where J is the current density, $Q_{j,v}$ is the volumetric source of current, σ is the electrical conductivity, E is the electric field, ω is the angular frequency, D is the electric displacement, J_e is externally generated current density, V is the electrical potential.

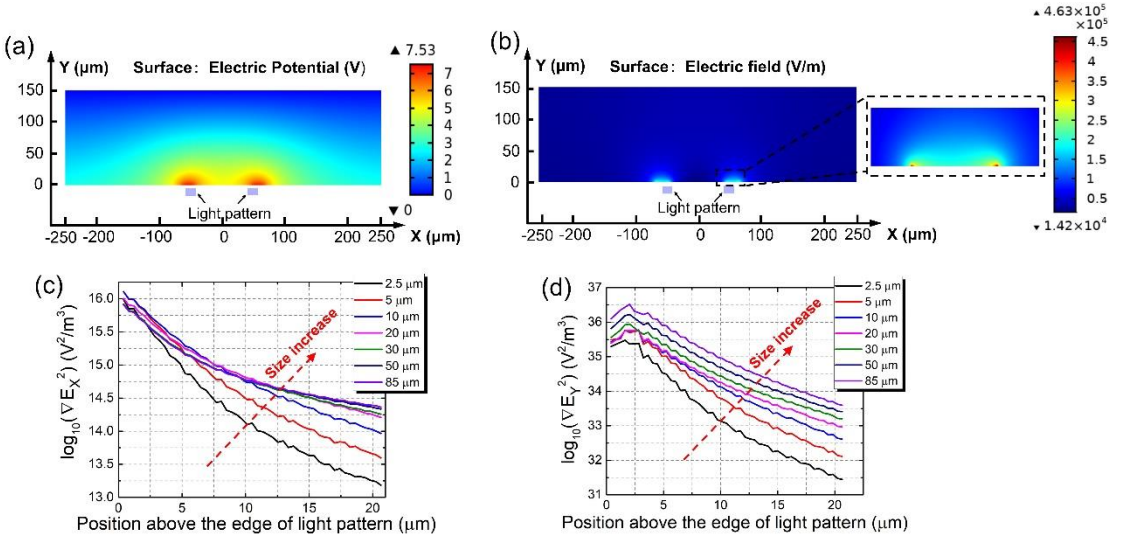

Figure 3. Plots for (a) simulated electric potential, and (b) simulated electric field for an OET trap formed by illuminating a light pattern on the photoconductive layer of an OET device. The simulated electric potential and electric field are plotted in heat maps (blue = low, red = high). The inset in (b) is a magnified

view of the main-panel data in the dashed square. Simulated gradients of electric field square (c) along X axis (horizontal plane), and (d) Y axis (vertical plane) above the edge of light patterns with different thickness (2.5-85 μm).

Shown in Figure 3(a) and (b) are the heat maps of the simulated electric potential and electric field distribution (i.e. cross-sectional view of an OET device). As shown, there is a big potential change at the edge of the light pattern resulting in a region of strong electric field with sharp field variation. This is caused by the difference in conductivity between the illuminated and dark a-Si:H surface. Since the bead reaches its maximum velocity at the edge of the light pattern, it is of great importance to investigate the DEP manipulation force exerted to the bead at the edge of the light pattern. Based on classic DEP theory for spherical microparticles,[36] the DEP force is given by:

$$F_{DEP} = 2\pi r^3 \varepsilon_m Re[K(\omega)]\nabla E^2 \quad (5.)$$

where r is the radius of the bead, ε_m is the permittivity of the medium, $Re[K(\omega)]$ is the real component of the CM factor, ∇E^2 is the gradient of the external electric field's square. Therefore, the DEP force exerted to the microbead is proportional to the gradient of electric field square (i.e. $F_{DEP} \propto \nabla E^2$). Based on the electric field distribution in Figure 3(b), the gradients of electric field square in X and Y directions (i.e. in horizontal and vertical planes) at the edge of the light pattern can be calculated for light patterns with different thickness, as shown in Figure 3(c) and (d), respectively. Based on the results in Figure 3(c), it can be inferred that the horizontal DEP force exerted to the bead increases as the light pattern thickness increases and the force saturates after the light pattern thickness reaches 20 μm. Besides, based on the results in Figure 3(d), it can be inferred that the vertical DEP force exerted to the bead increases as the light pattern increases and no sign of force saturation is observed. These simulation results provide important insights to the possible physical mechanism for the observed phenomenon on the moving behaviors of microbeads when they are manipulated by light patterns with different thickness. When the light pattern's thickness increases, the horizontal DEP force to balance the fluid viscous drag force also increases, therefore the maximum velocity of the bead increases along with the increase of the light pattern thickness. When the light pattern thickness increases to around 20 μm, the horizontal DEP force starts to saturate, resulting in the saturation of the bead's moving velocity. However, when the light pattern thickness increases to above 20 μm, the vertical DEP force continues to increases and the bead will experience stronger upward DEP force, which can lift the bead and make it escape with a hop. This interesting bead escaping behavior (i.e. the hopping behavior) has been investigated in our previous work and was shown mainly due to vertical DEP force.[38] Therefore, for light patterns above 20 μm, the induced horizontal DEP forces are similar but the induced vertical DEP forces are stronger for light patterns with larger thickness. As a result, the bead is more likely to be lifted up when manipulated by light patterns with larger thickness and thus can escape the OET trap at a slightly lower velocity. This explains why the moving velocity of bead increases to a peak and then start to decreases as the light pattern thickness increases (Figure 2).

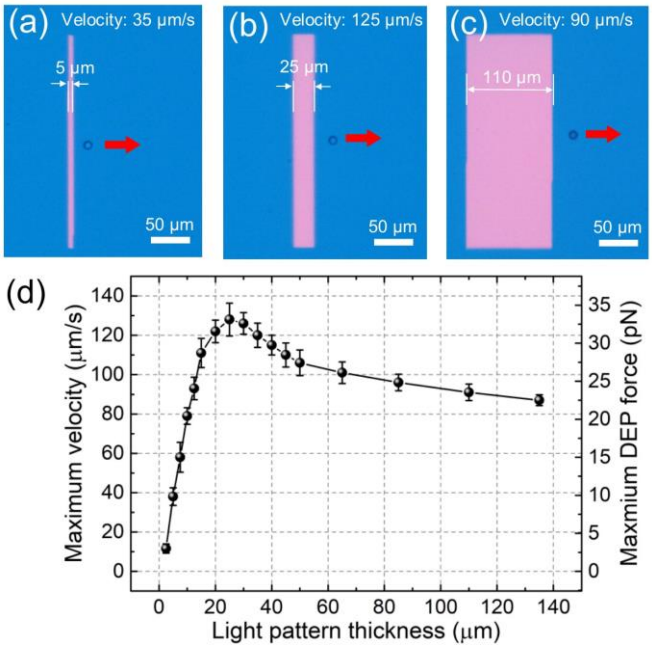

Figure 4. (a)-(c) Microscope images of a 10 μm polystyrene microbead trapped by rectangular-shaped light patterns with same length but different thickness (i.e. 5 μm, 25 μm and 110 μm), and moving at 35 μm/s, 125 μm/s and 90 μm/s, respectively. Red arrow represents the moving direction. (d) Maximum velocity and maximum DEP force versus light pattern's thickness. Error bars represent standard deviation for five replicates.

To test the universality of the physical mechanism, rectangular-shaped light patterns with fixed length at 270 μm but different thickness were used to manipulate a microbead, as shown in Figure 4(a)-(c) (worth noting that rectangular-shaped light patterns are widely used for cell/microparticle sorting in OET-integrated microfluidic devices[17,39-43]). The maximum velocity and maximum DEP force of the bead were measured/calculated accordingly, as shown in Figure 4(d). For a single microbead manipulated by rectangular-shaped light patterns with different thickness, its maximum velocity and maximum DEP force increase rapidly to a peak and then slightly decrease as the light pattern thickness increases from 2.5 μm to 135 μm. These results are similar to those observed experimentally for "doughnut"-shaped light patterns, suggesting the underlying physical mechanism a universal one that applies for light patterns with different shapes.

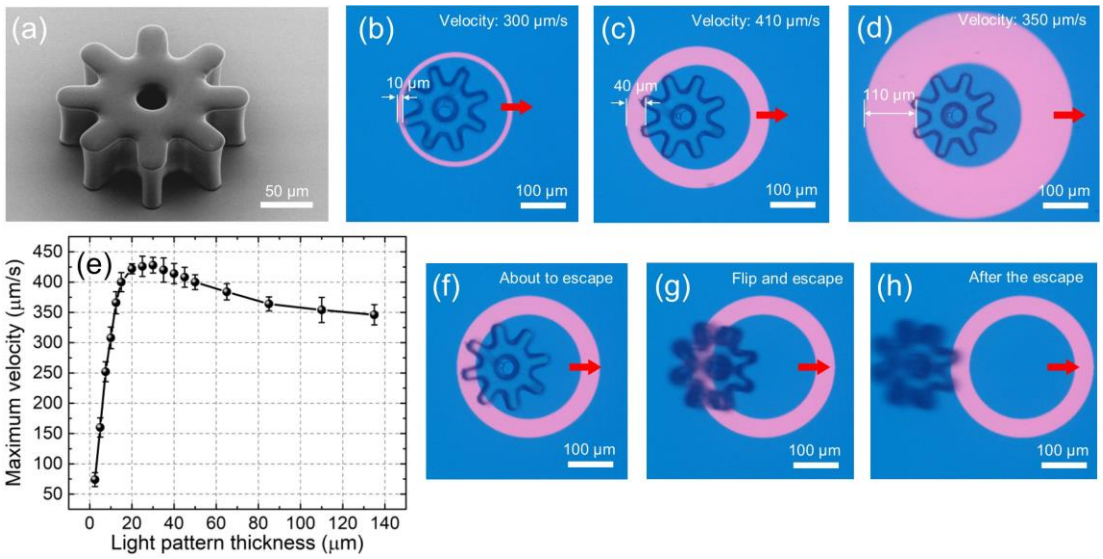

Figure 5. (a) SEM image of a micro-gear. (b)-(d) Microscope images of a micro-gear trapped by "doughnut"-shaped light patterns with same inner diameter but different ring thickness (i.e. 10 μm, 40 μm and 110 μm), and moving at 300 μm/s, 410 μm/s and 350 μm/s, respectively. Red arrow represents the moving direction. See Supplementary Video 3 (clip 1-3) for more details. (e) Maximum velocity of the micromotor versus light pattern's thickness. Error bars represent standard deviation for five replicates. (f)-(h) Microscope images showing the escape of a micro-gear from an OET trap with flipping behavior. See Supplementary Video 3 (clip 4) for more details.

Apart from microparticles, more experiments were carried out on other micro-objects, such as gear-shaped micromotors, as shown in Figure 5(a). The micromotor is made of SU8 materials and fabricated using standard photolithography technique.[9] It has a size of 200 μm and a height of 60 μm, much larger than the used 10 μm polystyrene microbead. The micromotor can be made to move at different velocities by "doughnut"-shaped light patterns with same inner diameter but different ring thickness, as shown in Figure 5(b)-(d) and Supplementary Video 3 (clip 1-3). The maximum velocity of the micromotor was measured for light patterns with different ring thickness, as shown in Figure 5(e). A similar trend was observed as for the cases with the microbeads, in which the maximum velocity increases to a peak and then slightly decreases as the light pattern thickness increases. These results demonstrate the universality of the physical mechanisms governing the moving behaviors of micro-objects regardless of the size, structure and material of the micro-objects when they are manipulated by OET with light patterns of different thickness. Shown in Figure 5(f)-(h) are microscope images of a micromotor escaping from a "doughnut"-shaped light pattern (from Supplementary Video 3 clip 4). Due to the vertical DEP force, the micromotor is lifted up and flip, and then escape the OET trap. These results help visualize the escaping behaviors of micro-objects in an OET system upon reaching its maximum moving velocity and also highlight the influence of vertical DEP force and related lifting effect on the micro-objects under OET manipulation.

In conclusion, we studied the influence of different light pattern thickness on the moving behaviors of microparticles and micromotors manipulated by OET. The experiments were supported by numerical simulations. It was found that the light pattern thickness can influence both the horizontal and vertical DEP forces significantly, leading to a first increase and then a decrease of the moving velocity of the micro-objects as the light pattern thickness increases. This work provides important information of optimizing light pattern parameters to achieve better OET performance for micromanipulation applications. In particular, users should consider both the horizontal and vertical DEP forces when selecting appropriate light pattern parameters to increase the moving velocities of micro-objects and exert stronger manipulation forces, which is important for improving OET performance for many applications.

Supporting Information

Descriptions of experimental setup, OET device structure and sample preparation are provided in the Supporting Information file.

Acknowledgements

This research was supported by the Natural Sciences and Engineering Research Council of Canada (Grant Nos. RGPIN 2019-04867, CREATE 482073-16, ALLRP 548593-19, and RTI-2019-00300), and National Natural Science Foundation of China (Grant Nos. 11774437, 61975243). The authors acknowledge the support from the Centre for Nanostructure Imaging at the Department of Chemistry, University of Toronto for assistance in collecting SEM images, and the Centre for Research and Applications in Fluidic Technologies (CRAFT) for assistance in micromotor fabrication. A.R.W. acknowledges the Canada Research Chair (CRC) program.

Author contributions

S.Z. conceived the idea, built the simulation model, and carried out the the experiments. S.Z. and M.E. built the experimental setup and fabricated the OET devices. Y.C. and Y.Z. deposited the a-Si:H materials. S.Z., S.L.N and A.R.W. wrote the manuscript. All authors discussed the results and commented on the manuscript. S.Z., S.L.N and A.R.W. coordinated and supervised the project.

Conflict of Interest

The authors declare no conflict of interest.

Reference

1. P. Y. Chiou, A. T. Ohta, and M. C. Wu, Massively parallel manipulation of single cells and microparticles using optical images, *Nature* 436, 370-372 (2005).
2. M. C. Wu, Optoelectronic tweezers, *Nat. Photonics* 5, 322-324 (2011).
3. M. Woerdemann, C. Alpmann, M. Esseling, and C. Denz, Advanced optical trapping by complex beam shaping, *Laser & Photon. Rev.* 7, 839-854 (2013).
4. Y. Huang, Z. Liang, M. Alsoraya, J. Guo, and D. Fan, Light-gated Manipulation of Micro/Nanoparticles in Electric Fields, *Adv. Intell. Syst.* 2, 1900127 (2020).

5. H. Hwang and J. K. Park, Optoelectrofluidic platforms for chemistry and biology, *Lab Chip* 11, 33-47 (2011).
6. S. Zhang, Y. Liu, J. Juvert, P. Tian, J. C. Navaro, J. M. Cooper, and S. L. Neale, Use of optoelectronic tweezers in manufacturing accurate solder bead positioning, *Appl. Phys. Lett.* 109, 221110 (2016).
7. S. Zhang, J. Juvert, J. M. Cooper, and S. L. Neale, Manipulating and assembling metallic beads with Optoelectronic Tweezers, *Sci. Rep.* 6, 32840 (2016).
8. S. Zhang, Y. Zhai, R. Peng, M. Shayegannia, A. G. Flood, J. Qu, X. Liu, N. P. Kherani, and A. R. Wheeler, Assembly of topographical micropatterns with optoelectronic tweezers, *Adv. Opt. Mater.* 7, 1900669 (2019).
9. S. Zhang, E. Y. Scott, J. Singh, Y. Chen, Y. Zhang, M. Elsayed, M. D. Chamberlain, N. Shakiba, K. Adams, S. Yu, C. M. Morshead, P. W. Zandstra, and A. R. Wheeler, The optoelectronic microrobot: A versatile toolbox for micromanipulation, *Proc. Natl. Acad. Sci. U.S.A.* 116, 14823-14828 (2019).
10. D. Han and J. K. Park, Optoelectrofluidic enhanced immunoreaction based on optically-induced dynamic AC electroosmosis, *Lab Chip* 16, 1189-1196 (2016).
11. D. Han and J. K. Park, Microarray-integrated optoelectrofluidic immunoassay system, *Biomicrofluidics* 10, 034106 (2016).
12. Y. H. Lin, C. M. Chang, and G. B. Lee, Manipulation of single DNA molecules by using optically projected images, *Opt. Expres*s 17, 15318-15329 (2009).
13. Y. Zhang, J. Zhao, H. Yu, P. Li, W. Liang, Z. Liu, G. B. Lee, L. Liu, W. J. Li, and Z. Wang, Detection and isolation of free cancer cells from ascites and peritoneal lavages using optically induced electrokinetics (OEK), *Sci. Adv.* 6, eaba9628 (2020).
14. S. Zhang, N. Shakiba, Y. Chen, Y. Zhang, P. Tian, J. Singh, M. D. Chamberlain, M. Satkauskas, A. G. Flood, N. P. Kherani, S. Yu, P. W. Zandstra, and A. R. Wheeler, Patterned optoelectronic tweezers: A new scheme for selecting, moving, and storing dielectric particles and cells, *Small* 14, 1803342 (2018).
15. S. Xie, X. Wang, N. Jiao, S. Tung, and L. Liu, Programmable micrometer-sized motor array based on live cells, *Lab Chip* 17, 2046-2053 (2017).
16. A. T. Ohta, M. Garcia, J. K. Valley, L. Banie, H. Y. Hsu, A. Jamshidi, S. L. Neale, T. Lue, and M. C. Wu, Motile and non-motile sperm diagnostic manipulation using optoelectronic tweezers, *Lab Chip* 10, 3213-3217 (2010).
17. S. B. Huang, M. H. Wu, Y. H. Lin, C. H. Hsieh, C. L. Yang, H. C. Lin, C. P. Tseng, and G. B. Lee, High-purity and label-free isolation of circulating tumor cells (CTCs) in a microfluidic platform by using optically-induced-dielectrophoretic (ODEP) force, *Lab Chip* 13, 1371-1383 (2013).
18. L. Y. Ke, Z. K. Kuo, Y. S. Chen, T. Y. Yeh, M. Dong, H. W. Tseng, and C. H. Liu, Cancer immunotherapy μ-environment LabChip: taking advantage of optoelectronic tweezers, *Lab Chip* 18, *106-114* (2018).
19. Y. Yang, Y. Mao, K. S. Shin, C. O. Chui, and P. Y. Chiou, Self-locking optoelectronic tweezers for single-cell and microparticle manipulation across a large area in high conductivity media, *Sci. Rep.* 6, 22630 (2016).
20. A. H. Jeorrett, S. L. Neale, D. Massoubre, E. Gu, R. K. Henderson, O. Millington, K. Mathieson, and M. D. Dawson, Optoelectronic tweezers system for single cell manipulation and fluorescence imaging of live immune cells, *Opt. Exp.* 22, 1372-1380 (2014).
21. A. Jamshidi, S. L. Neale, K. Yu, P. J. Pauzauskie, P. J. Schuck, J. K. Valley, H.-Y. Hsu, A. T. Ohta, and M. C. Wu, Nanopen: dynamic, low-power, and light-actuated patterning of nanoparticles, *Nano*

Lett. 9, 2921-2925 (2009).

22. S. J. Lin, S. H. Hung, J. Y. Jeng, T. F. Guo, and G. B. Lee, Manipulation of micro-particles by flexible polymer-based optically-induced dielectrophoretic devices, *Opt. Express* 20, 583-592 (2012).
23. M. B. Lim, R. G. Felsted, X. Zhou, B. E. Smith, and P. J. Pauzauskie, Patterning of graphene oxide with optoelectronic tweezers, *Appl. Phys. Lett.* 113, 031106 (2018).
24. S. Zhang, W. Li, M. Elsayed, P. Tian, A. W. Clark, A. R. Wheeler, and S. L. Neale, Size-scaling effects for microparticles and cells manipulated by optoelectronic tweezers, *Opt. Lett.* 44, 4171-4174 (2019).
25. M. A. Zaman, P. Padhy, Y. T. Cheng, L. Galambos, and L. Hesselink, Optoelectronic tweezers with a non-uniform background field, *Appl. Phys. Lett.* 117, 171102 (2020).
26. A. Jamshidi, P. J. Pauzauskie, P. J. Schuck, A. T. Ohta, P. Y. Chiou, J. Chou, P. Yang, and M. C. Wu, Dynamic manipulation and separation of individual semiconducting and metallic nanowires, *Nat. Photonics* 2, 86-89 (2008).
27. Y. H. Lin, K. S. Ho, C. T. Yang, J. H. Wang, and C. S. Lai, A highly flexible platform for nanowire sensor assembly using a combination of optically induced and conventional dielectrophoresis, *Opt. Express* 22, 13811-13824 (2014).
28. H. Hwang, D. Han, Y. J. Oh, Y. K. Cho, K. H. Jeong, and J. K. Park, In situ dynamic measurements of the enhanced SERS signal using an optoelectrofluidic SERS platform, *Lab Chip* 11, 2518-2525 (2011).
29. M. B. Lim, J. L. Hanson, L. Vandsburger, P. B. Roder, X. Zhou, B. E. Smith, F. S. Ohuchi, and P. J. Pauzauskie, Copper-and chloride-mediated synthesis and optoelectronic trapping of ultra-high aspect ratio palladium nanowires, *J. Mater. Chem. A* 6, 5644-5651 (2018).
30. S. Zhang, Y. Liu, Y. Qian, W. Li, J. Juvert, P. Tian, J. C. Navarro, A. W. Clark, E. Gu, M. D. Dawson, J. M. Cooper, and S. L. Neale, Manufacturing with light-micro-assembly of opto-electronic microstructures, *Opt. Express* 25, 28838-28850 (2017).
31. M. C. Tien, A. T. Ohta, K. Yu, S. L. Neale, and M. C. Wu, Heterogeneous integration of InGaAsP microdisk laser on a silicon platform using optofluidic assembly, *Appl. Phys. A* 95, 967-972 (2009).
32. J. Juvert, S. Zhang, I. Eddie, C. J. Mitchell, G. T. Reed, J. S. Wilkinson, A. Kelly, and S. L. Neale, Micromanipulation of InP lasers with optoelectronic tweezers for integration on a photonic platform, *Opt. Express* 24, 18163-18175 (2016).
33. Berkely Lights Inc. (https://www.berkeleylights.com/).
34. W. Liang, S. Wang, Z. Dong, G. B. Lee, and W. J. Li, Optical spectrum and electric field waveform dependent optically-induced dielectrophoretic (ODEP) micro-manipulation, *Micromachines* 3, 492-508 (2012).
35. J. K. Valley, A. Jamshidi, A. T. Ohta, H. Y. Hsu, and M. C. Wu, Operational regimes and physics present in optoelectronic tweezers, *J. Microelectromech. Syst.* 17, 342-350 (2008).
36. R. Pethig, Dielectrophoresis: Status of the theory, technology, and applications, *Biomicrofluidics* 4, 022811 (2010).
37. S. L. Neale, M. Mazilu, J. I. B. Wilson, K. Dholakia, and T. F. Krauss, The resolution of optical traps created by light induced dielectrophoresis (LIDEP), *Opt. Express* 15, 12619-12626 (2007).
38. S. Zhang, A. Nikitina, Y. Chen, Y. Zhang, L. Liu, A. G. Flood, J. Juvert, M. D. Chamberlain, N. P. Kherani, S. L. Neale, and A. R. Wheeler, Escape from an Optoelectronic Tweezer Trap: experimental results and simulations, Opt. Express 26, 5300-5309 (2018).

39. W. Liang, L. Liu, H. Zhang, Y. Wang, and W. J. Li, Optoelectrokinetics-based microfluidic platform for bioapplications: A review of recent advances, *Biomicrofluidics* 13, 051502 (2019).
40. Y. H. Lin and G. B. Lee, Optically induced flow cytometry for continuous microparticle counting and sorting, *Biosens. Bioelectron.* 24, 572-578 (2008).
41. C. Witte, J. Reboud, J. M. Cooper, and S. L. Neale, Channel integrated optoelectronic tweezer chip for microfluidic particle manipulation, *J. Micromech. Microeng.* 30, 045004 (2020).
42. T. K. Chiu, W. P. Chou, S. B. Huang, H. M. Wang, Y. C. Lin, C. H. Hsieh, and M. H. Wu, Application of optically-induced-dielectrophoresis in microfluidic system for purification of circulating tumour cells for gene expression analysis-cancer cell line model, *Sci. Rep.* 6, 32851 (2016).
43. W. P. Chou, H. M. Wang, J. H. Chang, T. K. Chiu, C. H. Hsieh, C. J. Liao, and M. H. Wu, The utilization of optically-induced-dielectrophoresis (ODEP)-based virtual cell filters in a microfluidic system for continuous isolation and purification of circulating tumour cells (CTCs) based on their size characteristics, *Sens. Actuators B Chem.* 241, 245-254 (2017).